

Synthesis of nano Lead Tungstate (PbWO_4) by Single Step Modified Combustion Process and Characterization for their application as LTCC and Optical Material

Bincy Joseph, Bincy Abraham and Jijimon K Thomas

Electronics Material Research Laboratory, Department of Physics, Mar Ivanios College(Autonomous), Thiruvananthapuram, Kerala, 695015, India.

Corresponding author:jkthomasemrl@yahoo.com

Abstract

Nanostructured Scheelite PbWO_4 were synthesized through a single step modified auto-ignition combustion technique. The X-ray diffraction, Fourier transform Raman and infrared spectroscopy studies revealed that the as-prepared samples were phase pure and the average crystallite size was ~ 49 nm. PbWO_4 crystallizes in tetragonal structure. The particle size and morphology of the sample was studied using transmission electron micrograph. The optical properties of the sample were studied using Ultraviolet-visible and photoluminescence spectra. The samples showed a maximum transmission in the visible regions but poor transmittance in the ultraviolet region. The optical band gap of the samples calculated using the Kubelka-Munk method was 3.87 eV, suggesting their semiconducting behavior. The photoluminescence spectra recorded on the samples showed that nano PbWO_4 has visible luminescence. The thermal stability of the sample at elevated temperatures has been studied using thermo gravimetric analysis (TGA) and differential thermal analysis (DTA). No substantive weight loss were observed for the samples in the temperature range 50-900°C. The PbWO_4 samples were sintered to 98% relative density at very low temperature of 787°C without using any sintering aid. The microstructure of the sintered pellets observed by Scanning Electron Micrograph (SEM) showed that the pellets were well sintered with minimum porosity. The dielectric constant (ϵ_r) of the sintered PbWO_4 sample was recorded using an LCR meter in the range 50 Hz to 5 MHz and showed a value of 86 at 1 MHz with a loss factor of 10^{-2} . The calculated



temperature coefficient of dielectric constant is negative. The low sintering temperature, dielectric constant, low loss factor and negative temperature coefficient make the sample ideal for low temperature co-fired ceramic, electronic substrate materials as well as suitable for various optical applications such as UV filters, transparent films for window layers on solar cells, anti-reflection coatings, scintillators, detectors.

Key words: PbWO_4 , LTCC, dielectric, sintering, combustion synthesis

Introduction

The emerging nano science and nanotechnology stimulate extensive research interest in nano structured metal oxides for potential applications. Particularly, the field of transition metal oxides represents an exciting and rapidly expanding research area that spans the border between the physical and engineering sciences. The main advantage of nano materials is that its properties can be fine-tuned with technical requirements. The better flexibility of nano materials to mould into different shapes and morphology compared with the bulk materials is an added advantage. Low temperature co-fired ceramic (LTCC) technology has attracted remarkable attention in fabrication of sensors and micro-fluidic devices in the last decade [1] and micro-channels are desired within the sensor module. Several works for the fabrication and on the study of LTCC material has been done [2-7].

PbWO_4 is an n-type semiconductor oxide material which is widely studied for their vast potential application in the various fields of science and technology. These oxides have drawn a great deal of attention of researchers due to its excellent electrochromic behaviour [8, 9], photochromic behaviour [10,11], gasochromic behavior [12, 13] and stability towards UV and visible region which could found wide range of applications in the field of electrochromic devices (ECD) [14, 15], memory devices [16,17], smart windows [18] catalytic material [19] and display applications [20]. They are also good gas sensors. PbWO_4 is most

attractive for its high-energy physics application because of its high density (8.4gm/cm^3), short decay time (less than 10 ns for a large light output), high irradiation damage resistance (10^7 rad for undoped), small moliereradius, fast decay time, non hygroscopicity and low production cost [21-22]. PbWO_4 shows interesting excitonic luminescence, thermoluminescence and simulated Raman scattering behavior [15-16]. Lead tungstate crystals are fast and dense scintillators found an application for high energy electromagnetic calorimeter of Compact Muon Solenoid (CMS) detector at Large Hadron Collider (LHC) at Center of Europe for Research Nuclear(CERN).

Synthesis and characterization of snowflake-like and bamboo- leaf like PbWO_4 nanocrystals was successfully demonstrated [23]. A study on the properties of lead tungstate crystals, the longitudinal optical transmittance and light attenuation length, light yield and response uniformity, emission spectra and decay time was investigated [24]. The radiation resistance of large crystals and possible curing with optical bleaching are discussed. The results of an in depth materials study, including trace impurities analysis, are also presented. The general conclusion from this investigation is that further research and development is needed to develop fast, radiation hard PbWO_4 crystals for the CMS experiment at the CERN LHC.

Experimental

Synthesis

In the present work, nanopowder was prepared through a modified combustion process. As usual procedure, in combustion technique, alcohol was used as the complexing agent and fuel respectively. In such case high temperature annealing of the as-prepared powder was required to get a phase pure powder [25-28]. But in the present modified combustion method, citric acid was used as the complexing agent instead of poly vinyl alcohol. By this change of complexing agent it is

possible to obtain single phase nanoparticles in a single step combustion process without the usual calcinations for prolonged duration at high temperature. The main advantage of this method is that the as prepared powder itself shows phase formation. Single step process, i.e. no pre or post calcinations is required. Same fuel + oxidizer + complexing agent combination can be used to prepare simple oxides, perovskites, mixed oxides, ceramics, aluminates, ferrites, hafnates, scheelites etc. As prepared powder itself is phase pure. Narrow particle size distribution and uniform morphology. Particle size, composition and homogeneity of the products can be controlled. No particular heating rate is needed, no special crucibles or containers or arrangements are required. Easy to handle and economical both in cost and time.

In the present work we have synthesized single phase Nano Lead Tungstate using a modified combustion technique. Lead Nitrate and Ammonium paratungstate dissolved in double distilled water were used as starting reagent for the preparation of nanocrystalline PbWO_4 . Citric acid was then added to the solutions taken in separate beakers as complexing agent. Amount of citric acid was calculated based on total valence of the oxidizing and the reducing agents for maximum release of energy during combustion. Oxidant to fuel ratio of the system was adjusted to unity (~ 1) by adding concentrated nitric acid which serves as oxidizer and ammonium hydroxide solution as fuel. The precursor solution of pH ~ 7.0 was stirred well for uniform mixing without any precipitation or sedimentation. The solution was then heated using a hot plate kept at $\sim 250^\circ\text{C}$ in a ventilated fume hood. The solution boils on continuous heating and undergoes dehydration accompanied by foam. On persistent heating the foam gets auto-ignited giving a voluminous fluffy powder of nano PbWO_4 . The structure of the as-prepared powder was examined by the powder x-ray diffraction (XRD) technique using a Philip Pro X-ray diffractometer with $\text{CuK}\alpha$ radiation as the incident beam. The infrared (IR) spectra of the samples were recorded on a Perkin

Elmer spectrum 2 instrument recording a wavelength ranging from 375-2500 cm^{-1} and it consist of an optimized KBr beam splitter. The Fourier-transform Raman spectrum of the nanocrystalline PbWO_4 was measured at room temperature in the wavenumber range from 50 cm^{-1} to 1200 cm^{-1} using a Bruker RFS/100S spectrometer at power level of 150mW and resolution of 4 cm^{-1} . Particulate properties of the combustion product were observed using transmission electron microscopy (TEM, model JEOL-JEM 2100 with an accelerating voltage of 200 kV). The samples were excited using a Nd:YAG laser lasing at 1064 nm, and the scattered radiation was detected using a Ge detector. The photoluminescence spectra of the samples were measured using a Horiba Scientific Fluoromax-2 Spectrofluorometer and was studied between the wavenumber 310 cm^{-1} to 600 cm^{-1} . The photons from the source were filtered by an excitation spectrometer. The monochromatic radiation was then allowed to fall on the disc samples, and the resulting radiation was filtered by an emission spectrometer and then fed to a photomultiplier detector. The variation of intensity was recorded as a function of wavelength. Optical measurements of the nanopowder were performed at room temperature using a PERKIN ELMER λ -35, Singapore, is used for recording a wavelength ranging from 150-700 nm. The same solvent was used as blank for analysis to calibrate the spectrophotometer. To study the sinterability of the nanoparticles obtained by the present combustion method, as-prepared PbWO_4 nanoparticles were mixed with 5% polyvinyl alcohol and pressed in the form of cylindrical pellets of 12 mm diameter and 2 mm thickness at pressure of about 150 MPa using a hydraulic press. The pellet was then sintered at 787°C for 3 h (Standard four probe technique using Keithley source meter 2440). The surface morphology of the sintered sample was analyzed using scanning electron microscopy (SEM model JEOL-JSM 5610 LV, Tokyo, Japan). For low-frequency dielectric studies, pellets were made into the form of a circular disc capacitor with the specimen as the dielectric medium. Both of the flat surfaces of the sintered pellet were polished and electroded by applying silver paste. The capacitance of

the sample was determined using an LCR meter (3532-50 LCR Hi-Tester; Hioki) in the frequency range from 100 Hz to 5 MHz at different temperatures from 30°C to 500°C.

Results And Discussion

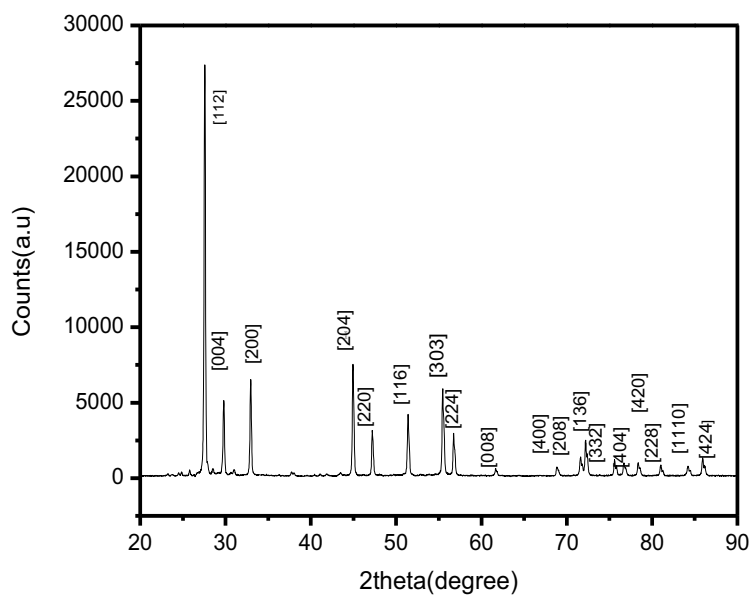
Structural Analysis

XRD patterns of the synthesized nanoparticles using combustion method with ammonia as fuels. All the peaks were indexed for their (h, k, l) planes in the spectrum. No secondary phase was seen in the XRD pattern which confirms that powder itself is phase pure. But the XRD of the as prepared sample showed the presence of some organic and other impurity peaks and hence the sample was annealed at 700°C.

The XRD pattern of PbWO_4 nanopowder is shown in Figure 1. All the diffraction peaks were assigned to Scheelite phase with tetragonal structure with space group ($I4_1/a$ [88]), JCPDS card No. 19-0708. The lattice parameters calculated from XRD pattern are $a = 5.432 \text{ \AA}$, $b = 5.432 \text{ \AA}$, $c = 12.064 \text{ \AA}$ for PbWO_4 which are well agreeing with the standard value reported. The crystallite size is calculated from full width at half maximum (FWHM) of the peak using Scherrer formula. The average crystallite size of the as prepared sample is 49 nm. The description about the structure, crystallite size, lattice parameter of the sample is enclosed in Table 1. The highest relative intensity is obtained for [1 1 2] crystallographic plane of tetragonal crystal structure of Scheelite phase.

Table 1:

Compound	Crystal Structure	Lattice parameter						Unit cell volume (Å) ³	Crystallite size (nm)
Lead Tungstate	Tetragonal	Standard (Å)			Calculated (Å)			355.96	49
		A	B	C	a	b	C		
		5.461	5.461	12.049	5.432	5.432	12.064		

Figure 1: XRD pattern of PbWO_4 nanopowder.

The extent of line broadening in the diffraction pattern due to the strain, which is caused by the non-uniform displacement of the atoms with respect to their reference lattice position, could be identified by Williamson–Hall (W–H) method [29]. Figure 2 shows the Williamson–Hall plot for the PbWO_4

nanoparticles. The reciprocal of 'y' intercept, a measure of particle size, obtained from this plot was 45nm. The lattice strain constant 'g', proportional to the slope of the line, estimated as 5.76×10^{-5} . The positive slope of the line indicates that strain is tensile and is also a component contributing to the broadening of peaks in the XRD pattern.

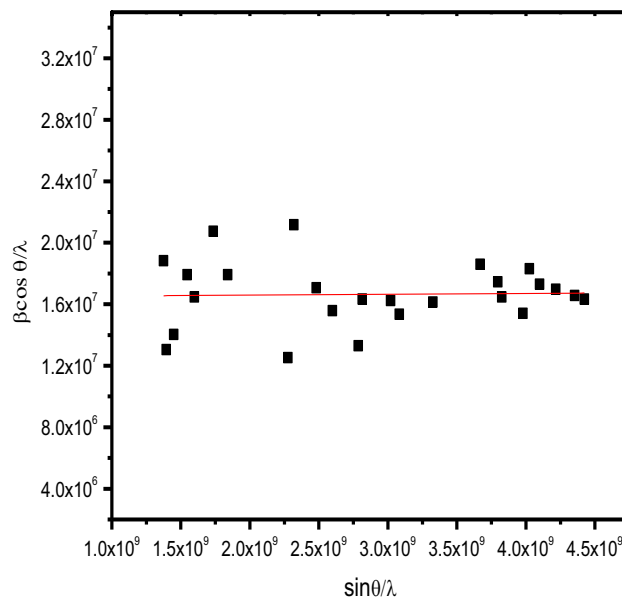


Figure:2 Williamsons Hall plot of nano PbWO₄

FT-IR spectra of the sample are recorded and are given in Figure 3. In the scheelite structure, W ions are in tetrahedral O⁻ ion cages and isolated from each other. Each Pb²⁺ cation is surrounded by eight oxygen ions. The connection between cation Pb²⁺ and anion WO₄⁻² is ionic and the connection between W⁶⁺ and O²⁻ in the oxyanion complex is covalent. The W atom in the scheelite structure is at the tetrahedral O-atom cages and isolated from one another and the number of O ion surrounding each Pb ion is eight. Figure 4 shows the FTIR spectra of the PbWO₄ lead tungsten nanoparticles. The observed absorption

peaks are in good agreement with the earlier reports [30]. The FTIR spectra indicate an intense band around 729 cm^{-1} . This band is due to the W-O-W stretching vibration modes, characteristic of tetrahedral tungstate [31, 32]. The broadness of this band is attributed to the characteristic nano nature of the lead tungstate crystals.

$$\Gamma_{Td} = A_1(\nu_1) + E(\nu_2) + F_2(\nu_3) + F_2(\nu_4)$$

in which all four vibrational modes are Raman active, Figure (3.13), but only the $F_2(\nu_3, \nu_4)$ modes are IR active [33, 34]. The band at 729 cm^{-1} are assigned to $F_2(\nu_3)$ antisymmetric stretches vibrations for PbWO_4 .

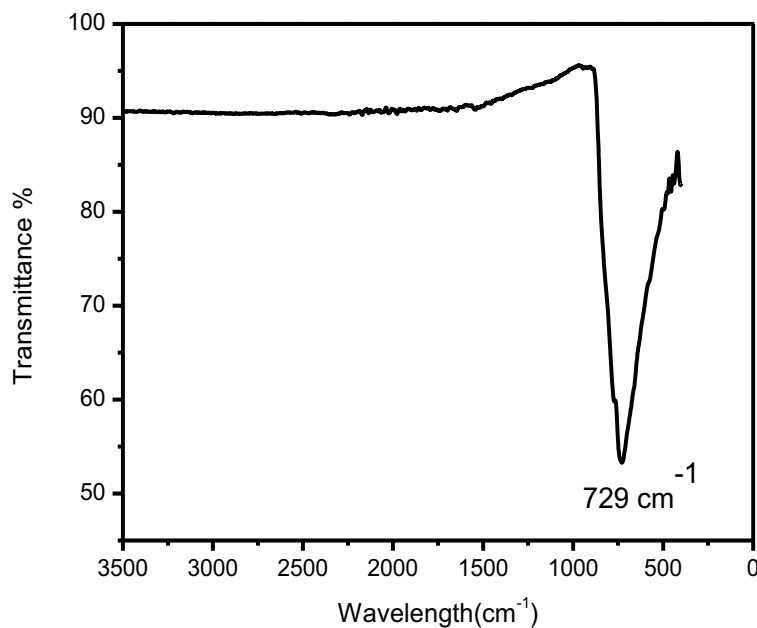


Figure 3. FT-IR Spectra of nano PbWO₄

PbWO₄ crystallizes at ambient conditions in the centro symmetric scheelite structure that has the space group (I4_{1/a})[88], with four formula units per body-centered unit cell. The Pb and W atoms occupy S₄ sites whereas the sixteen oxygen atoms are on general C₁ sites. Group theoretical considerations [35-37] lead us to expect 13 Raman active modes at the τ point [38].

$$\tau = \nu_1(A_g) + \nu_2(A_g) + \nu_2(B_g) + \nu_3(B_g) + \nu_3(E_g) + \nu_4(B_g)$$

$$+ \nu_4(E_g) + R(A_g) + R(E_g) + 2T(B_g) + 2T(E_g). \text{-----}(3)$$

The translational modes (T) and the rotational modes (R) are considered to be the external modes of the WO₄ tetrahedra and are the lowest in frequency. The rest [(ν_1) to (ν_4)] are considered to be the internal modes of the WO₄ tetrahedra and higher in frequency. The A_g and B_g modes are single, while E_g modes are doubly degenerated [39].

To the best of our knowledge twelve of the thirteen modes of the scheelite-type phase of PbWO₄ are known [40,41] the (ν_4) E_g internal mode being the only unknown one. This mode has been observed in CaWO₄, SrWO₄ and BaWO₄ as a high-frequency shoulder of the (ν_4) B_g internal mode [37,40,41].

Figure.4 shows the Raman spectrum of Scheelite nano PbWO₄. The Raman spectrum of scheelite is dominated by the (ν_1) A_g mode near 903 cm⁻¹. The peaks in the range 600–1000 cm⁻¹ were assigned to the stretches of the W–O bonds. The W–O bonds of intermediate length (about unit valency) are characteristic of bridging W–O bonds and are assigned to Raman mode stretching wavenumbers in the range 700–1000 cm⁻¹. The bands at 764, 715 cm⁻¹ and 806, 845 cm⁻¹ are assigned to F₂(ν_3) antisymmetric stretches vibrations for PbWO₄ [42-50].

A higher Raman stretching mode wavenumber indicates a more distorted

structure, whereas a lower Raman stretching mode wavenumber indicates a more regular structure [51]. PbWO_4 present a strong peak at 800 cm^{-1} , the W–O bond of WO_4 tetrahedral in PbWO_4 catalysts [52-54]. Table 2 encloses the Raman band assignments of nano PbWO_4 .

Table.2:

PbWO ₄ assignments (cm ⁻¹)	Raman band assignments
63	T(E _g)
75	T(B _g)
88	T(E _g)
176	R(A _g)
325	ν_2 (A _g)
355	ν_4 (B _g)
750	ν_3 (E _g)
903	ν_1 (A _g)

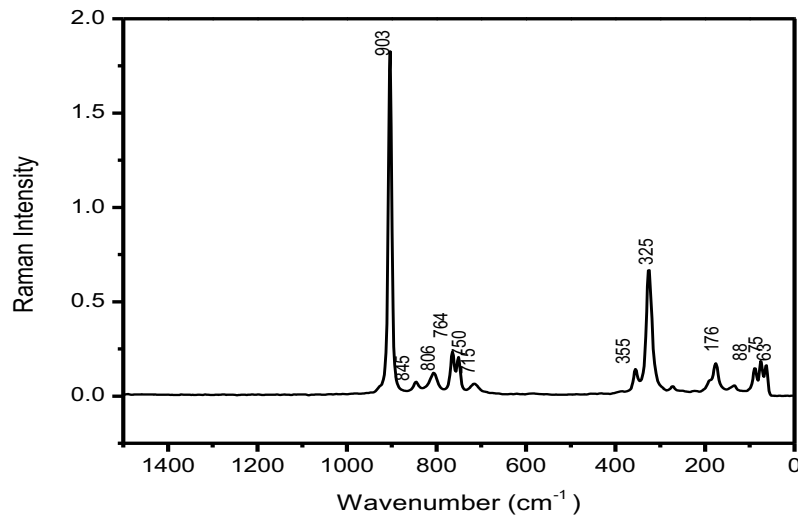


Figure.4 Raman spectra of nano PbWO₄

Powder Morphology

TEM images of the PbWO₄ samples prepared via solution combustion processes annealed at 700°C are given in Figure 5[a] and 5[b]. From the distinctly visible grains, the average grain size is calculated as 24 nm. Corresponding to (1 1 2) plane of tetragonal crystal structure of PbWO₄ the interplanar spacing obtained from X-Ray diffraction plane is found to be in good agreement with the interplanar spacing, 0.322 nm for the same plane obtained from TEM image. The d-spacing for different crystallographic planes estimated from Figure 5[a] matches well with the d-spacing obtained from X-ray diffraction analysis.

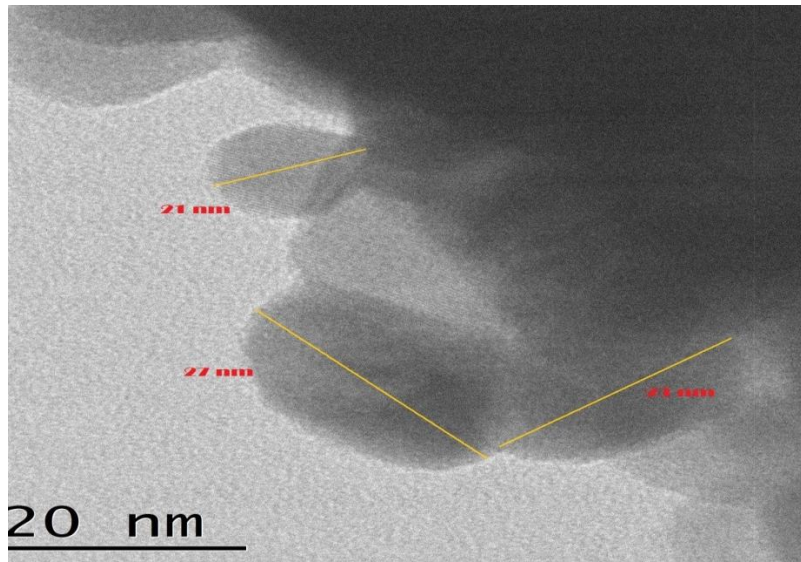


Figure.5(a) HRTEM image of a single grain

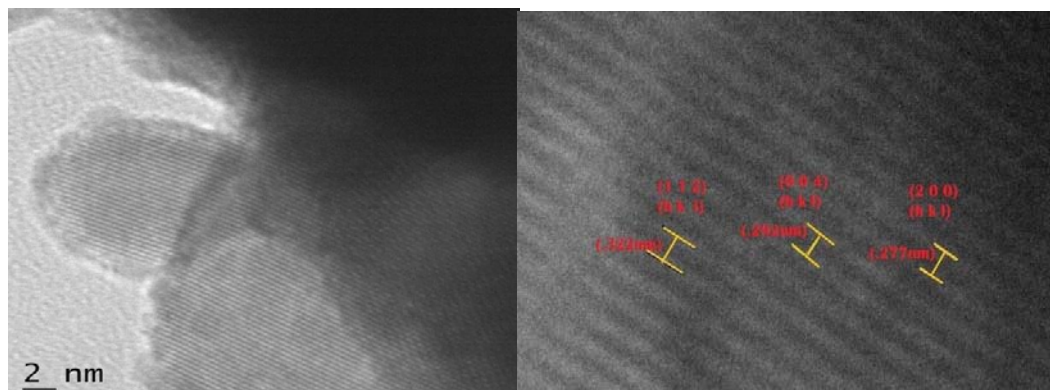


Figure.5(b) HRTEM image of different crystallographic planes.

Figure 6 shows the TGA/DTA curve of nano PbWO_4 , in the temperature range from 30°C to 900 °C at a heating rate of 10 °C in nitrogen atmosphere. It shows no significant weight loss throughout from ambient to 900 °C. The TGA curve shows that the particles crystallize at room temperature itself and the thermal stability of the nanostructures are really good. No abrupt changes are observed in the TGA curve in the higher temperature range which indicate that no phase transitions are occurring and the PbWO_4 ceramics synthesized by the modified combustion synthesis is stable at elevated temperature range [23,55].

The DTA graph shows a small endothermic dip around 100 °C and 790 °C attributes to the evaporation of the absorbed moisture and the melting of PbWO_4 powder respectively, which is noted during the sintering of PbWO_4 powder

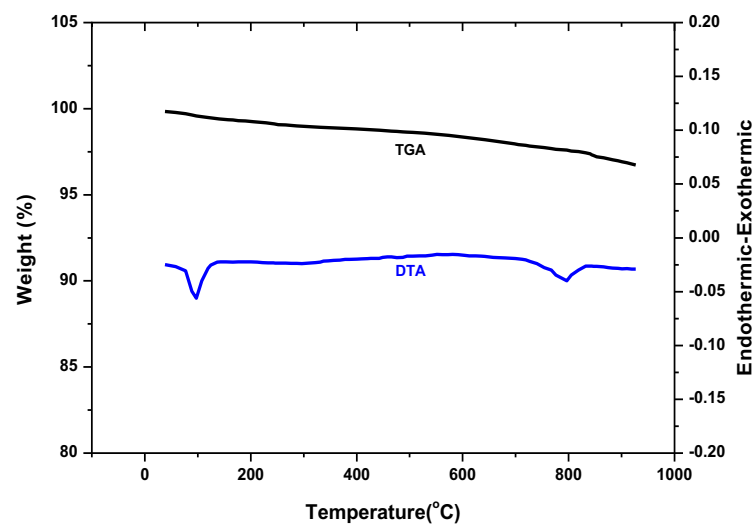


Figure: 6 TGA/DTA Curve of nano PbWO_4

Optical Study

The UV-Visible absorption, reflectance and transmission spectra of nano PbWO_4 are shown in the Figure 7[a], 7[b] and 7[c] respectively. Sample shows maximum absorption in the UV region with a steep absorption edge centered at 364 nm. This absorption is attributed to a charge transfer transition in which an oxygen 2p electron goes into one of the empty tungsten 5d orbital [55]. The excitation from O_{2p} to W_{t2g} in the WO_4^{2-} group absorbs ultraviolet irradiation in PbWO_4 . In the excited state of the WO_4^{2-} groups, the hole (on the oxygen) and the electron (on the tungsten) remain together as an exciton because of their strong interactions [56-58]. The maximum absorbance occurred within the UV region from where the absorbance decreased with the wavelength towards the visible region. PbWO_4 showed intense and narrow band. The transmittance increased

exponentially from the UV region towards the visible region. The transmission spectrum showed that the sample exhibits very high transmittance in the visible region. The properties of poor transmittance in the UV but high transmittance in the visible regions makes this sample excellent materials in screening off UV portion of electromagnetic spectrum which is dangerous to human health. A film of this material can be used for coating eye glasses for protection from sunburn caused by UV radiations. The reflectance spectra of the samples had a maximum hike at the UV region. Maximum absorption in the UV region along with uniform transparency in the visible region makes the sample ideal for UV sensors, filters and screening applications. Also, the property of high transmittance and low reflectance in the visible region makes the material a good candidate for transparent windows in solar cells.

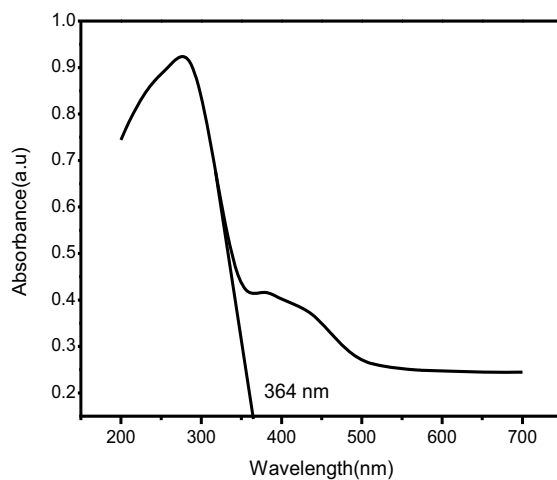


Figure 7[a]. UV-Absorbance graph of nano PbWO₄

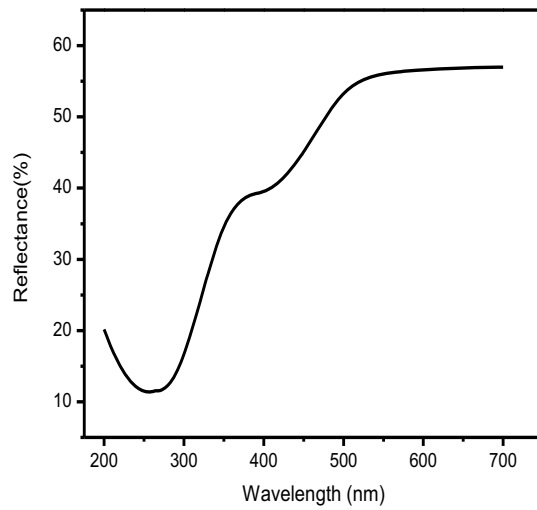


Figure: 7[b]. Reflectance graph of nano PbWO₄

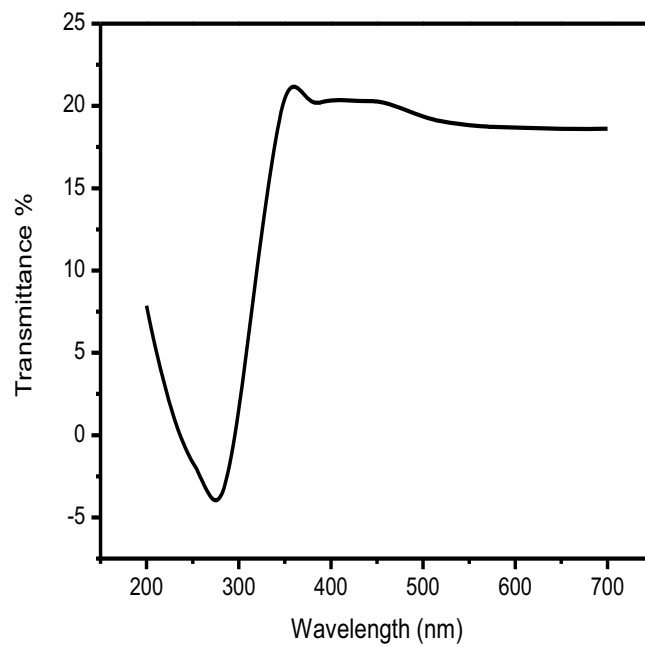


Figure: 7[c]. Transmittance spectra of nano PbWO₄

A semiconductor is characterized by its electronic band structure. In the high energy absorption region, the dependence on the photon energy is expressed by Tauc's equation. The Wood and Tauc [59,60] equation was used to estimate the optical band gap of nano PbWO₄ powder. According to this equation, the optical band gap energy is related with absorbance and photon energy by the following equation:

$$\alpha h\nu = (\beta h\nu - E_g)^m$$

where " β " is an energy independent constant, α is the optical absorption coefficient, " h " is the Planck's constant, ν is the frequency of incident photon, " E_g " is the optical band gap and " m " is a constant which characterizes the nature of band transition. $m = 1/2$ and $3/2$ corresponds to direct allowed and direct forbidden transitions and $m = 2$ and 3 corresponds to indirect allowed and indirect forbidden transitions, respectively. The optical band gap can be obtained from the extrapolation of the straight-line portion of the $(\alpha h\nu)^{1/m}$ versus $h\nu$ plot to $\alpha h\nu = 0$. The existence of sharp absorption band is an indication of excellent crystalline nature of the nanosample. The calculated optical band gap is illustrated in Figure 8. The band gap of the sample is found to be 3.87 eV, which is matching with the value reported [23] for PbWO₄. The present obtained value is lower than that reported by [61] which is 4.1 eV. The lowering of band gap can be due to several factors such as changes in local atomic structure, lowering of symmetry of lattice, electro negativity of transition metal ions, connectivity of the polyhedrons, deviation in the O–X–O bonds, oxygen vacancies, distortion of the [XO₄]²⁻ tetrahedrons and intrinsic surface states [23,61]. As the band gap is the energy difference between valance and conduction band, the presence of these intermediate levels resulted in the reduction of optical band gap energy. As PbWO₄ prepared by the present method possess wide band gap along with good transmittance in the visible region is suitable for transparent conducting oxide films for window layers on solar cells.

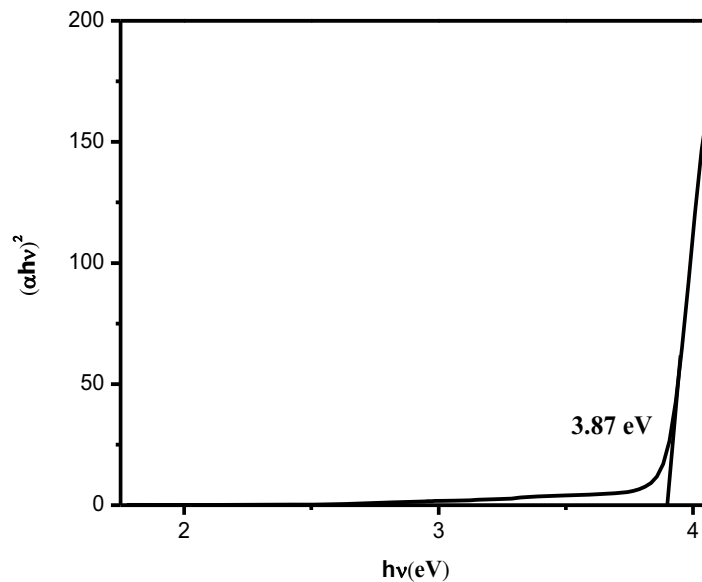


Figure:8 Tauc's plot of nano PbWO₄

Figure.9 shows the photoluminescence spectra of nano PbWO₄. Scheelite phase of PbWO₄ give rise to the blue luminescence at 450 nm, when excitation energy in an exciton band region around (250-330nm). This luminescence has been regarded as being an intrinsic feature of Scheelite phase of PbWO₄. In our case a broad emission band at 370–600 nm with maximum emission at 479 nm is observed. The luminescence is ascribed to the radiative decay of self-trapped excitons in regular WO₄²⁻ group. The blue emission is due to transitions in the regular tungsten [WO₄²⁻] group in which Pb²⁺ play a role [23]. There are two defects: 1) A regular lattice (WO₄²⁻) defect and 2) Defect based on WO₃ center, which are responsible for the complex character of PbWO₄ emission. The blue emission is an intrinsic feature of PbWO₄ and is generally ascribed to the radiative decay of self-trapped exciton that locates on the regular WO₄ group [23]. The green luminescence is of

extrinsic origin and it was ascribed to a defect based WO_3 center possibly with F center. The concentration of these defects are strongly influenced by the raw material and the method used for the crystal growth. According to the band theory given [62], the bottom of conduction band is formed by both 5d state of W^{6+} ion and 6p state of Pb^{2+} ion in PbWO_4 and the coping of valence band is formed by both 6s state of the Pb^{2+} ion and the 2p state of O^{2-} ion. The W_{5d} states are degenerated and split in a crystal field of tetragonal symmetry in e and t_2 vibrational modes. The Pb 6s state and Pb 6p state have appreciable contribution throughout the valence band and conduction band respectively. When PbWO_4 is excited within fundamental absorption band charge transfer by two types of electronic transition can be observed

- a. From O^{2-} to W^{6+} within WO_4^{2-} oxyanion complex
- b. From O^{2-} to Pb^{+2} outside WO_4^{2-} oxyanion complex.

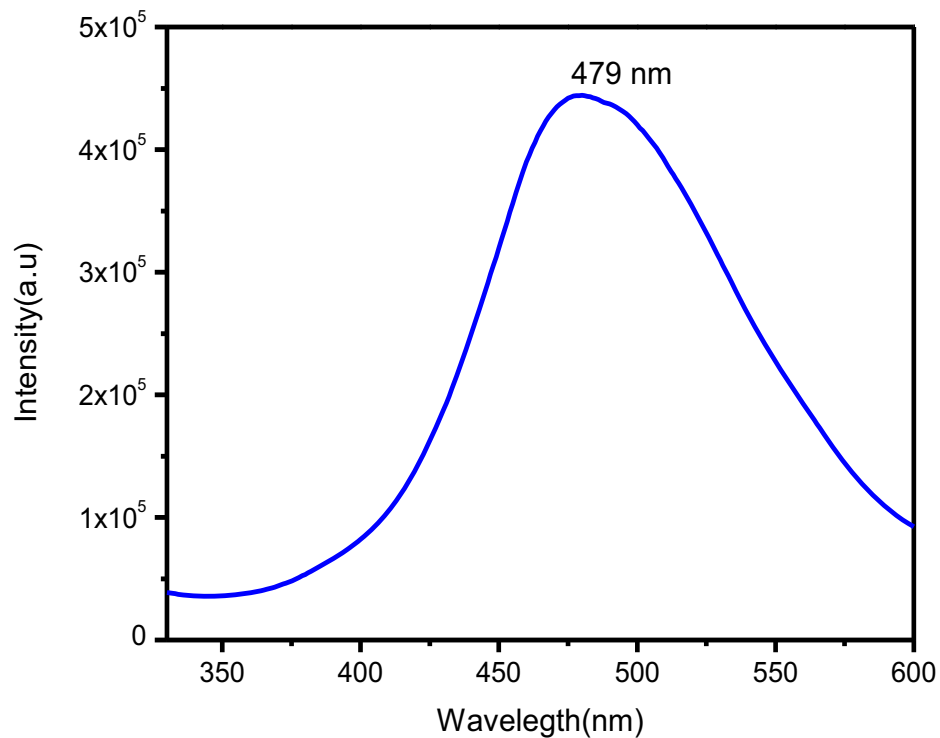


Figure.9 Photoluminescence spectra of nano PbWO₄

Sintering And Dielectric Behavior

After several trials, the sintering temperature of compacted nanopowders of PbWO₄ were optimized. The relative green density of the specimen used for the sintering study was 72%. The sample was sintered at 787⁰C for 3 hours at a rate of 10⁰C/minute without using any sintering aid. The density of the sintered sample calculated by Archimedes method is 98%. Figure.10, depicts that the attempts to increase the density by increasing the temperature or soaking time led to the melting of the pellets. So the optimized sintering temperature and time is 787⁰C for 3 h. The high sintered density for PbWO₄ pellets derived from nano powder was obtained through the agglomeration, ultra fine nature of the powder and grain

boundary diffusion. Figure.11[a] and Figure.11[b] shows the photograph of green and sintered pellets respectively. From the photographs the change in the colour of the pellet from pale yellow to crimson yellow can be noted which is the characteristic feature of the sample nano PbWO_4 . Lead and oxygen vacancies are generally created due to the Pb and O deficiency in the PbWO_4 crystal. These vacancies are responsible for colour centres in this crystal [63]. The colour of the crystal is also influenced by the pre-annealing time before melting of initial powder [64].

To the best of our knowledge the sintering of the sample nano PbWO_4 at a lower temperature of 787°C has not been accomplished before.

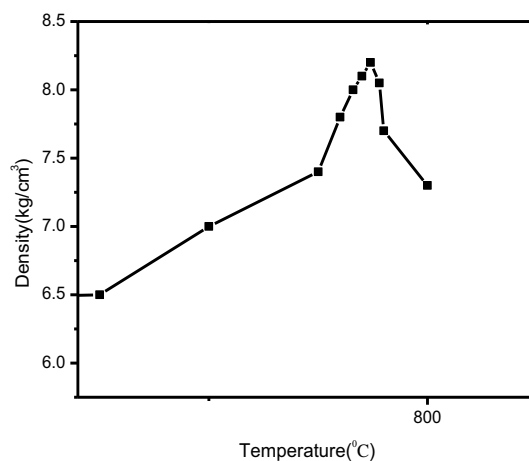


Figure.10: Variation in density with sintered temperature

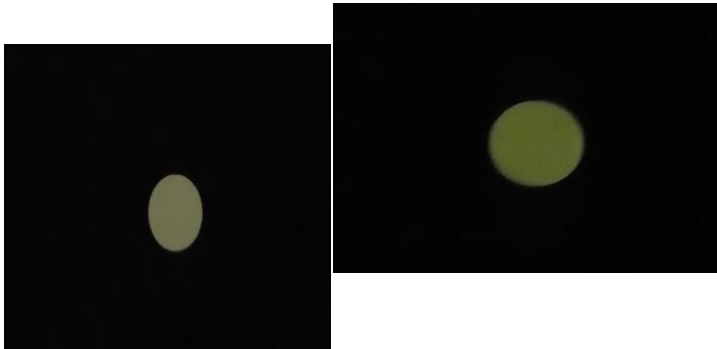


Figure.11[a]: Photograph of Green Pellet

Figure.11[b]: Photograph of Sintered Pellet

The highly dense sintered pellet was hand polished and then thermally etched at 680°C for an hour in air. The surface morphology of the sintered pellet was studied using Scanning Electron Microscopy. Figure.12 is the SEM micrograph of the sintered pellet, which indicates that the pellet is well sintered with negligibly minimum porosity. It is also noticeable that the sample has attained appreciable density and also the grain boundaries are clear cut which indicates that the sample is not in melt phase. It is observed from the micrograph that the size of the grains has increased from 500 nm to about $5\mu\text{m}$ due to sintering.

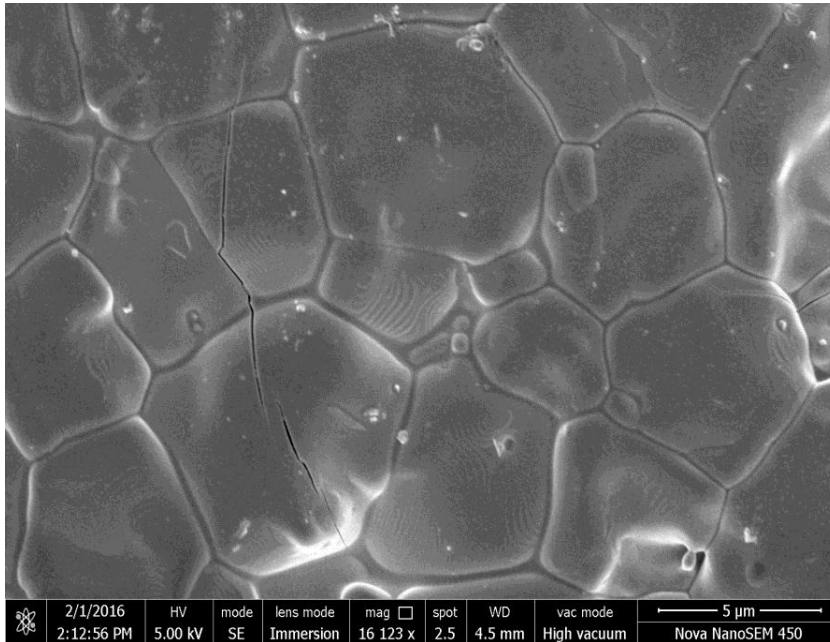


Figure.12: Scanning Electron Micrograph of nano PbWO₄

The dielectric constant ϵ_r and loss factor $\tan\delta$ values of the pellet sintered from the nanopowder, synthesized through the above combustion process were studied in the frequency range 100 Hz to 5 MHz at room temperature with silver electrodes on both sides of the circular disc. Figure.13[a] and Figure.13[b] shows variation of dielectric constant and $\tan\delta$ with the frequency respectively. The dielectric constant ϵ_r and loss factor $\tan\delta$ values of the PbWO₄ pellets at 1 MHz are 86 and 1×10^{-2} respectively. Figure.14 shows the variation of dielectric constant at different temperature at constant frequency of 1 MHz. The values of dielectric constant and very low loss factor indicate the suitability of the sample as a candidate for electronic and dielectric application. It is clear from the graph that the temperature dependence of dielectric constant is very minimal in the measured range. The loss factor decreases with increase of temperature and is of the order 1×10^{-2} at temperature above 100°C. The temperature coefficient of dielectric constant ($T_c k$)

is determined using the equation given below between temperature 500°C and 30°C at 5MHz.

$$T_c K = \left[\frac{K_{500} - K_{30}}{220} \right] \times 10^6 \text{ ppm/}^\circ\text{C}$$

where K_{30} and K_{250} are dielectric constants at 30°C and 500°C respectively, and 220 is the temperature difference. The obtained $T_c K$ is

-13 ppm/°C which is negative. The value of dielectric constant at room temperature was found to be 86 and was observed that the value of dielectric constant at higher temperature from 30°C to 500°C remained constant without much variation. Thus nano PbWO_4 possess relatively low temperature coefficient of dielectric constant which makes it suitable for temperature dependent dielectric applications.

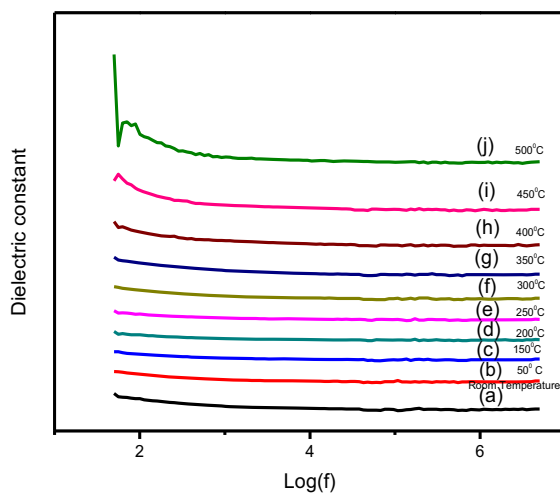


Figure.13[a]: Variation of dielectric constant with frequency of sintered PbWO_4 pellet at temperatures (a) Room temperature (b) 50°C (c) 150°C (d) 200°C (e) 250°C (f) 300°C (g) 350°C (h) 400°C (i) 450°C (j) 500°C

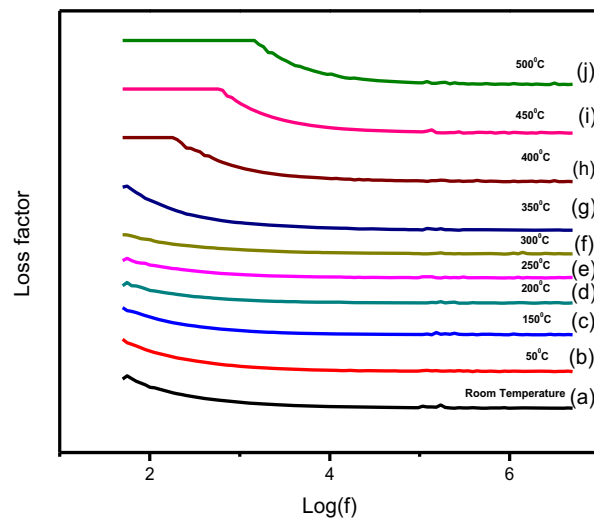


Figure.13[b]: Variation of loss factor with frequency of sintered

PbWO_4 pellet at temperatures (a) Room temperature (b) 50°C
 (c) 150°C (d) 200°C (e) 250°C (f) 300°C (g) 350°C (h) 400°C
 (i) 450°C (j) 500°C

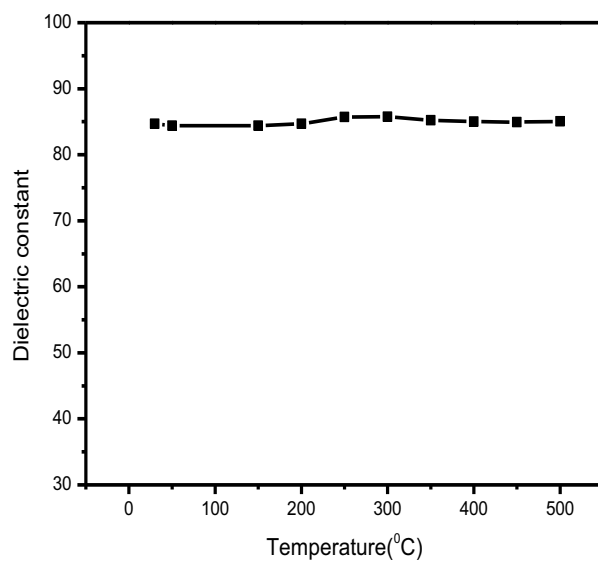


Figure.14: Variation of Dielectric constant with temperature at 1kHz.

Conclusion

Nanostructured Scheelite PbWO_4 compound prepared by the present technique come under the category of Low Temperature CoFired Ceramics (LTCC) materials as the sintering temperature is as low as 787^0 C. Usually glass and polymer composite materials are used for LTCC application. But their high dielectric loss compose restrictions on their effective use as LTCC materials. The low value of sintering temperature makes PbWO_4 samples a promising material for LTCC application, substrate application and electronic packaging materials. It may be noted in the present study we have succeeded in developing PbWO_4 samples, which is sintered nearly 400^0C lower than the sintering temperature reported for their conventional powders, without use of any sintering aid. Also the sample possess excellent dielectric and optical behavior which makes this material a promising candidate for LTCC and optical applications.

Reference

1. E. Khoo, P.S. Lee, J. Ma, J. Euro. Ceram. Soc. 30 ,2010.
2. S. Vidya, Sam Solomon, J. K. Thomas., Synthesis, Characterization, and Low Temperature Sintering of Nanostructured BaWO_4 for Optical and LTCC Applications, 2013.
3. S. Vidya, Sam Solomon, J.K. Thomas., Synthesis of Nanocrystalline CaWO_4 as Low-Temperature Co-fired Ceramic Material, 2013.
4. S. Vidya, Sam Solomon, J. K. Thomas., Processing, Structural and

Physical Properties Nanocrystalline scheelite SrWO_4 : a low temperature

Co-Fired ceramic optical material-synthesis and properties, 2013.

5. S. Vidya, Sam Solomon, J.K. Thomas., Structural, optical and dielectric characterization of nanocrystalline $\text{AMo}_{0.5}\text{W}_{0.5}\text{O}_4$ (where A=Ba, Sr and Ca) prepared by single step modified combustion technique, 2015.
6. S. Vidya, Sam Solomon, J. K. Thomas., Synthesis and characterization of MoO_3 and WO_3 nanorods for low temperature co-fired ceramic an optical applications, Springer Science, Business Media New York, 2015.
7. S Vidya, K C Mathai, Annamma John, Sam Solomon, K Joy, J. K Thomas., Optical and dielectric properties of nano BaNbO_3 prepared by a combustion Technique, 2013.
8. N. Oka, M. Watanabe, K. Sugie, Y. Iwabuchi, H. Kotsubo, Y. Shigesato., Thin Solid Films, 2013.
9. Yi Shen, Rong Huang, Yang Li, Shuzhen Yao., Appl. Surf. Sci., 2011.
10. A.I. Gavriluk., Appl. Surf. Sci., 2013.
11. A. Georg, W. Graf, R. Neumann, V. Wittwer., Sol. Energy Mater. Sol. Cells, 2000.
12. N. Tahmasebi Garavand, S.M. Mahdavi, A. Irajizad, M. Ranjbar., Sens. Actuator B Chem., 2012.
13. S. Papaefthimiou, G. Leftheriotis, P. Yianoulis., Thin Solid Films, 1999.
14. K. Kuribayashi, H. Harigae, Y. Suzuki, Y. Uchida., Energy Procedia, 2012.
15. K.S. Yook, S.O. Jeon, C.W. Joo, J.Y. Lee, S.H. Kim, J. Jang., Org. Electron. 10, 2009.
16. A. Kuzmin, A. Anspoks, A. Kalinko, J. Timoshenko, R. Kalendarev., J. Non-Cryst. Solids 401, 2014.
17. K.A. Gesheva, T.M. Ivanova, G. Bodurov., Prog. Org. Coat. 74, 2012.
18. H. Liu, Z. Ma, Y. Chu, W. Sun., Colloid Surf. A 287, 2006.

19. L. Wang, X. Wei, Y. Luo, J. Yuan, Y. Ding., Displays 32, 2011.
20. P.Lecoq, IDafinei, E Auffray, M Schneegans, V Korzhik, O V Missevitch, V. B Pavlenko, AAFedorov, A N Annenkov, V L Kostylev., Nucl. Instrum.Meth. A
21. M Kobayashi, M Ishii, Y Usuki., Nucl.Instrum Methods Phys .Res.,1998.
22. K Hara, M Ishii, M Usuki., Y NuclInstrum.methods Phys.Res,1998.
23. T. George, S. Joseph, A. T. Sunny, S. Mathew., Morphology Tuning of Tungstate Nanostructures bySoft Chemistry., Journal Of Nanoparticles
24. R.Y. Zhu a, D.A. Maa, H.B. Newman,C.L. Woodyb, J.A. Kiersteadb, S.P. Stollb, P.W. Levy ., A study on the properties of lead tungstate crystals., A California Institute of Technology, 1996
25. K. C. Patil., Advanced ceramics: combustion synthesis and properties .,Bulletin of Materials Science, vol. 16, no. 6.
26. K.C Patel, M.SHegde, Tanu Rattan, S T Aruna., Chemistry of Nanocrystalline oxide materials Combustion synthesis properties and application., World Scientific Publishing, 2008.
27. Kashinath C. Patila, S.T. Aruna, TanuMimani., Combustion synthesis: An update., Current Opinion in Solid State and Materials Science 6, 2002.
28. K.C.Mathai, S. Vidya, S. Solomon, J.K Thomas., Variation in Optical, dielectric and sintering behavior of nanocrystallineNdBa₂NbO₆, Adv. Mater. Res., An Intl Journal.No. 2.

29. G.K. Williamson, W.H. Hall, X-Ray line broadening from filed aluminium and wolfram, *Acta Metall.* 1 ,1953.
30. P.H. Bottlebergs, H. Everts, G.H.J. Broers., *Mater. Res. Bull.*, 11 ,1976.
31. A.M. Golub, V.I. Maksin, A.A. Kapshuk, S.A. Kirillov.,*Russ. J. Inorg. Chem.*, 21 ,1976 .
- 32 . D. L. Rousseau, R. P. Baumann, and S. P. S. Porto., *J. Raman Spectrosc.*,1981.
33. S. P. S. Porto and J. F. Scott., *Phys. Rev.* 157,1967.
- 34.G. Herzberg., *Molecular Spectra and Molecular Structure: II Infra-Red and Raman Spectra* _D. Van Nostrand Co. Inc., NewYork, 1945.
35. F. J. Manjón, D. Errandonea, N. Garro, J. Pellicer-Porres, P.Rodríguez-Hernández, S. Radescu, J. López-Solano, A. Mujica, A. Muñoz., *Phys. Rev. B* 74 ,2006.
36. F. J. Manjon,D. Errandonea, N. Garro, J. Pellicer-Porres, J. López-Solano, P. Rodríguez-Hernández,S. Radescu, A. Mujica, A., Muñoz, Lattice dynamics study of scheelitetungstates under high pressure II. PbWO_4 .,*Physical Review B* 74 ,2006.
37. Burcham, L. J, Wachs, I. E., Vibrational analysis of the twonon-equivalent, tetrahedral tungstate (WO_4) units in $\text{Ce-2(WO}_4\text{)(3)}$ and $\text{La-2(WO}_4\text{)(3)}$. *Spect. Acta Part A*, 1998.
38. Nakamoto, K., *Infrared, Raman Spectra of Inorganic, Coordination Compounds*, 4th edn.Wiley, New York, 1996.
39. S. P. S. Porto and J. F. Scott., *Phys. Rev.* 157,1967.
- 40.G. Herzberg., *Molecular Spectra and Molecular Structure: II Infra-Red and Raman Spectra* _D. Van Nostrand Co. Inc., NewYork, 1945.
41. F. J. Manjón, D. Errandonea, N. Garro, J. Pellicer-Porres, P.Rodríguez-Hernández, S. Radescu, J. López-Solano, A. Mujica, A. Muñoz., *Phys. Rev.*

- B 74,2006.
42. F. J. Manjon, D. Errandonea, N. Garro, J. Pellicer-Porres, J. López-Solano, P. Rodríguez-Hernández, S. Radescu, A. Mujica, A., Muñoz, Lattice dynamics study of scheelitetungstates under high pressure II. PbWO_4 , Physical Review B 74,2006.
43. J. M. Stencel, J. Springer, and E. Silberman., J. Mol. Struct., 1977.
44. S. Bastians, G. Crump, W. P. Griffith, R. Withnall., J. Raman Spectrosc,2004.
45. D. Christofilos, K. Papagelis, S. Ves, G. A. Kourouklis, C. Raptis., J. Phys.: Condens. Matter ,2002.
46. D. Christofilos, S. Ves, and G. A. Kourouklis., Phys. Status Solid B, 1996.
47. A. N. Akimov, M. V. Nikanovich, V. G. Popov, and D. S. Umreiko., J. Appl. Spectrosc,1987.
48. N. Weinstock, H. Schulze, and A. Müller., J. Chem. Phys,1973.
49. J. M. Stencel, J. Springer, and E. Silberman., J. Mol. Struct., 1977.
50. S. Bastians, G. Crump, W. P. Griffith, R. Withnall., J. Raman Spectrosc,2004.
51. D. Christofilos, K. Papagelis, S. Ves, G. A. Kourouklis, C. Raptis., J. Phys.: Condens. Matter ,2002.
52. D. Christofilos, S. Ves, and G. A. Kourouklis., Phys. Status Solid B, 1996.
53. A. N. Akimov, M. V. Nikanovich, V. G. Popov, and D. S. Umreiko., J. Appl. Spectrosc,1987.
54. N. Weinstock, H. Schulze, and A. Müller., J. Chem. Phys,1973.
55. H. Fu, J. Lin, L. Zhang, Y. Zhu., Appl. Catal. A, 2006.
56. M. J. J. Lammers, G. Blasé, D. S. Roberson., Phys. Status Solidi A, 1981.

57. F. Lei, B. Yan, H-H. Chen, Q. Zhang, J-T.Zhao.,Cryst. Growth & Des., 2009.
58. V.B. Mikhailik, H. J. Kraus., Appl. Phys., 2005.
59. D.L. Wood and J. Tauc., Phys. Rev. B 5, 3144 ,1972.
60. D. L. Wood and J. Tauc., Weak absorption tails in amorphous semiconductors, Physical Review B, vol. 5, no. 8, pp,1972.
61. Y. Zhang, N.A.W. Holzwarth, R.T. Williams., Phys. Rev. B, 57,1998.
62. F. Lei, B. Yan, H-H. Chen, Q. Zhang, J-T.Zhao.,Cryst. Growth & Des., 2009.
63. N. Nikl, K. Nitsch, S. Baccaro, B. Borgia, M. Martini, M.Kobayashi, M. Ishii, Y. Usuki, O. Jarolimek, P. Reiche.,J. Appl. Phys. ,1997.
64. D.H. Kim, H.S. Yang, K.D. Chang, H.Y. Park, M.B. Lee, J.H. Lee, Y.H. Song, Y.R. Cho, S.Y. Lee, J. Crystal Growth,2001.